JOURNAL OF MECHANICAL ENGINEERING, SCIENCE, AND INNOVATION
ITATS
Research Article

Numerical Performance of Four-Wheeled Cruise-controlled Vehicle on Road Surface

Journal of Mechanical Engineering, Science, and Innovation
e-ISNN: 2776-3536
2023, Vol. 3, No. 2
DOI: 10.31284/j.jmesi.2023.v3i2.5310
ejurnal.itats.ac.id/jmesi

Desmas Arifianto Patriawan[1], Ahmad Anas Arifin[2], and Bambang Pramujati[3]

[1]Peneliti Mandiri Mekatronika, Indonesia
[2]Mechanical Engineering Department, Institut Teknologi Adhi Tama Surabaya, Indonesia
[3]Mechanical Engineering Department, Institut Teknologi Sepuluh Nopember, Indonesia

Corresponding author:
Desmas Arifianto Patriawan
Peneliti Mandiri Mekatronika, Indonesia
Email: patriawan87@gmail.com

Abstract

Cruise control (CC) has started to be widely used in cars, making driving easier for a long time. However, in designing the control system on the CC, it is also necessary to perform performance testing, so that the CC can achieve the desired speed accurately and comfortably. The approach employed in this paper involves creating a numerical model design based on CC and subsequently assessing its performance through simulations with varying levels of resistance. Variation of resistance given is by road conditions (rolling resistance) and drag coefficient. The test outcomes, when subjected to changes in road surface conditions, demonstrate that CC remains capable of achieving a rapid response time and maintaining a consistent steady-state error of approximately 2.01%. Despite minimal variations observed in the drag coefficient test, the CC-designed model remains dependable in accommodating alterations in road surface and discrepancies in drag coefficients. Furthermore, the resultant vehicle acceleration does not exceed 2G, ensuring passenger comfort is not compromised.

Keywords: *Cruise control, Drag coefficient, Rolling resistance, Steady-state error, Time response*

Received: November 27, 2023; Received in revised: January 8, 2024; Accepted: January 9, 2024
Handling Editor: Hasan Maulana

INTRODUCTION

Congestion is a problem in transportation. One of the causes of congestion is skill in driving. Human driving involves reaction times, delays and human errors [1]. These three problems can affect traffic flow. When the traffic flow is problematic, congestion will

occur. In addition, careless human driving can lead to accidents. In Indonesia, accidents occur because of collisions, and the cause is people's non-compliance while driving [2]–[4]. The human error factor can be overcome with autonomous vehicles.

Autonomous vehicles are still at level 3, requiring a human role in control. The Society of Automotive Engineers (SAE) has standardized the level of autonomous vehicles from level 0 to level 5 [5]. Level 0, where the vehicle is fully controlled by humans, and level 5, where the system controls the vehicle [6]. The design that needs to be considered is the autonomous vehicle information system and dynamics. In terms of information, it is important for autonomous vehicles to have accurate and precise navigation [7]; apart from that, sensors and good communication systems between vehicles, roads and transportation infrastructure are also needed. Sensors are needed for autonomous vehicles to move safely. There are about nine types of sensors needed. Each of them have different needs to carry out autonomous functions [8]. Braking using the Anti-lock Braking System (ABS) is also needed to be developed as a safety system for driving [9].

The first step in developing autonomous vehicles is the development of cruise control (CC). The development and testing of CC have existed since 1993 when the development of this CC became autonomous intelligent cruise control (AICC). The results of implementing the AIC system have the potential to produce better traffic flow when compared to without using AICC [1]. The addition of communication devices between vehicles can also improve the performance of the CC. Improving the CC system with vehicle communication produces a Cooperative Adaptive Cruise control (CACC) system. The CACC system produces a more optimal and safer distance between vehicles due to communication between vehicles so that the system can predict and provide optimal and safe distances [10], [11]. In addition, the development of CC for various types of terrain is also needed to prevent accidents when the friction coefficient between the wheels and the road changes [12]. In this paper, we develop a CC system that is adaptive to changes in vehicle resistance. Resistance to vehicles can occur due to differences in friction efficiency between the tires and the road and air resistance hitting the vehicle body.

METHODS AND ANALYSIS

This research uses numerical modelling to get test results. Modelling needs to be done because testing the cruise control system with variations in friction efficiency can be dangerous. However, in subsequent studies, experimental testing can be carried out. Modelling is done to get the effect of changes in the friction coefficient on the CC system and how the control system can improve the vehicle's response to disturbances from changes in the friction coefficient.

In vehicles, the friction coefficient occurs on the tires, where the friction will affect the vehicle's acceleration. Vehicle acceleration will also affect the response of the CC. In simple terms, the acceleration of the vehicle can be written as:

Where m is the vehicle's mass, a is the vehicle's maximum acceleration, μ is the coefficient of friction between the tires and the road, and N is the vehicle's normal force from the vehicle's mass with gravity. Then the result of the equation is:

$$m\,a = \mu\, mg \tag{1}$$

Since m is the mass of the vehicle, the acceleration is:

$$a = \mu\, g \tag{2}$$

However, the value of μ can change with the condition of the vehicle and the road. If the vehicle is about to move, the static friction coefficient that occurs is μ_s, and if the vehicle has started moving, then the dynamic friction coefficient is μ_d. Regarding the tire

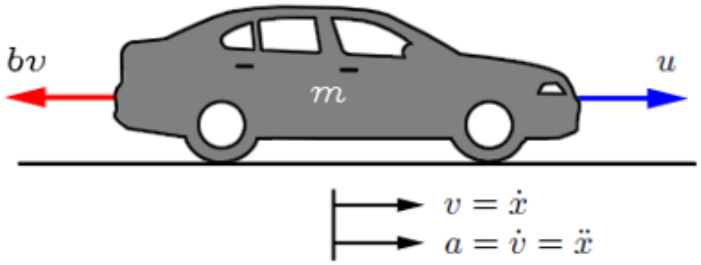

Figure 1. Free body diagram of the vehicle

Table 1. Several types of rolling coefficients (μ_r)

No	Type of road and tires being measured	Rolling resistance coefficients
1	Vehicle tires on new asphalt	0.01-0.015
2	Vehicle tires on asphalt	0.02
3	Vehicle tires on a cobble	0.03
4	Vehicle tires on solid sand	0.04-0.08

mechanism, getting a grip is not as easy as in equation (3). The grip a tire gains is derived from the mechanical motion between the tire and the road, the chemical bond between the tire and the road, temperature, tire pressure, ambient conditions, tread design and the tire's compounds [13]. These eight factors affect the grip force, which affects the value of μ.

In this paper, the coefficient of friction used is the coefficient of rolling resistance, μ_r, which can be obtained from:

$$\mu_r = F/G \tag{3}$$

Where F is the horizontal force exerted on the tire, while G is the vertical load received by the tire [14]. The coefficient of rolling resistance can be defined as a dimensionless parameter [15], so that if there is a difference in angle β between the road and the tires, then μ_r can be calculated in this way:

$$\mu_r = \tan\beta \tag{4}$$

The value of the coefficient of rolling resistance can be obtained using measurement. Methods for measuring rolling resistance values include drum test of tires, trailer method, coast-down methods and fuel consumption methods [16]. Various measurement methods will produce different coefficient values. Accurate measurements need to be made to get the rolling resistance value without any other influencing factors because a reduction in the rolling resistance value will affect energy savings [17]. Table 1 shows the rolling friction coefficients.

The rolling coefficients in Table 1 will have different values if used on vehicles. The difference in these values is influenced by tire pressure (p) and vehicle velocity (v). So that the rolling coefficient on the vehicle (μ_{rv}) can be calculated by

$$m_{rv} = \mu_r + (1/p)(0.01 + 0.0095(v/100)^2 \tag{5}$$

The results in Table 1 may change if accurate dynamic material property measurements are obtained, knowledge of the finite element model in each rubber product and optimization of tire construction. The rolling resistance will decrease if these three actions are carried out continuously [18]. Rolling resistance testing already has a

standard. The standards used are ISO-28585 and ISO-18164, which are then compared with the SAE-J1269 and SAE-J2452 standards. From this test, the results obtained have the same correlation despite several different parameters. These results prove that if you use one of the test standards and get improvements, testing with other standards produces almost the same results [19]. The results obtained in Table 1 are the rolling resistance used with almost the same method used by SAE-J1269 and SAE-J2452.

From equation (6) it can be calculated the force resulting from the tire's rolling resistance. The rolling resistance force is obtained as follows.

$$F_r = \mu_{rv}\, m\, g \tag{6}$$

The smaller the rolling resistance (F_r), the better, making the vehicle more efficient. In addition, the difference in F_r will be used as a variable to test the reliability of the control system on CC.

In addition to rolling resistance, the drag force on the vehicle is also influenced by the drag force F_d. The following equation obtains the drag force.

$$F_d = C_d\, \frac{1}{2}\rho v^2 A \tag{7}$$

Where C_d is the drag coefficient, ρ is the density of the fluid, v is the flow velocity, and A is the characteristic of the frontal area of the vehicle body. The drag coefficient will differ depending on the surface area of the particles and changes in the flow pattern around the particles [20], [21]. Changes in the flow pattern of the particles make the Reynolds Numbers (Re) also change, so the drag coefficient on non-spherical particles is obtained.

$$C_d = \frac{30}{Re} + \frac{67.289}{\exp(5.03\,\varphi)} \tag{8}$$

Where φ is the division result of the irregularly shape particle (S), divided by the actual surface area of the particle (S_d) so that $\varphi = {}^{S}/_{S_d}$ [22].

The resistance force in the vehicle can be caused by two factors, namely, the rolling resistance force and the drag force that exists on the vehicle. The resistance force on the vehicle can be calculated by

$$F_v = F_r + F_d \tag{9}$$

The resulting resistance force will affect the vehicle's mileage because it becomes a damping coefficient. So that the change in the resistance force to the damping coefficient in the modelling can be obtained by the equation

$$b_v = \frac{F_v t}{m} \tag{10}$$

Where t is the length of time the vehicle has been running, and s is the distance the vehicle has travelled. The resulting damping coefficient will be a barrier to the vehicle's speed to reach the speed setpoint determined by CC.

Cruise control (CC) on vehicles must be designed to produce vehicles with the right transient response and minimal steady-state errors. The exact transient state response to CC depends on internal and external factors. The internal factors that affect the transient response of the CC are mass, inertia and friction. While the external factor is the ever-changing road conditions, so if it has a fast transient response, it can also be dangerous if the road conditions are congested, slippery and bumpy. However, from several previous studies, the transient response needed to achieve an increase in speed between 15-25

m/s requires 5-10 seconds [1], [11], [23], [24]. These results are also used as a reference for assessing the performance of the transient response in designing control systems. Meanwhile, the steady-state error should not be more than 10%; this percentage must be smaller than in previous studies [12], [24].

Proportional, integral and derivative (PID) controllers are used to design the control system of the CC. PID controllers have been used since 1939 in the industrial sector [25] because the simple structure, ease of implementation and robustness make the PID controller still relevant [26]. Simple parameters, such as the position of an object over time, can be controlled with a PID controller [27], [28]. In addition, the advantages of the PID controller can be combined and developed with other controller methods, especially to dampen vibrations [29], [30].

PID controller is a form of parallel controller consisting of proportional P, integral I and derivative D. In its use, it is not necessary to use the three parameters depending on the plant and the results of the response from the system. The PID controller equation in parallel can be seen:

$$u(t) = K_c(e(t) + \frac{1}{T_i}e(t) + T_d\frac{de(t)}{dt}) \quad (11)$$

Where the proportional gain is $K_p = K_c$, the integral time is T_i and $K_i = \frac{K_c}{T_i}$. Derivative time is T_d and $K_d = K_cT_d$. In tuning the PID controller, it can be done with First Order Plus Time Delay (FOPTD), where there are two main parameters. The first parameter is related to the closed-loop time constant, and the second is the robustness level [31]. The development of PID controller tuning can also be combined with the classic tuning method integrated into intelligent control [26], [32]. The method of this integration process will be carried out later to get the tuning value of the PID controller. However, using a PID controller also has weaknesses in the dynamic testing of induction motors [33]; these results will be a note for future research.

Modelling Parameters

The modelling parameters used in this paper can be seen in Table 2. The empty mass of the vehicle is 1045 kg, but it is filled with 7 passengers so the total mass can be seen in Table 2. Simulink modelling is then made from these parameters, which can be seen in Figure 2.

The vehicle plant is then given a PID controller to get the desired speed (setpoint). PID tuner is used to get its proportional, integral and derivative values. However, adjustments need to be made so that acceleration is measured because large acceleration causes passengers to experience G-forces and can experience motion sickness. There are

Table 2. Modelling parameters used

Input Parameter	Dimensions	Value
Mass vehicle	kg	1535
Vehicle Power	kW	78.3
Initial velocity	m/s(km/h)	11.11(40)
Final velocity	m/s(km/h)	30.56(110)
Force $\boldsymbol{F_{r1}}$ on an asphalt road	Newton	300.86
Force $\boldsymbol{F_{r2}}$ on a cobble	Newton	451.29
Force $\boldsymbol{F_{r3}}$ on solid sand	Newton	902.58
$\boldsymbol{F_d}$ on vehicle	Newton	217.5

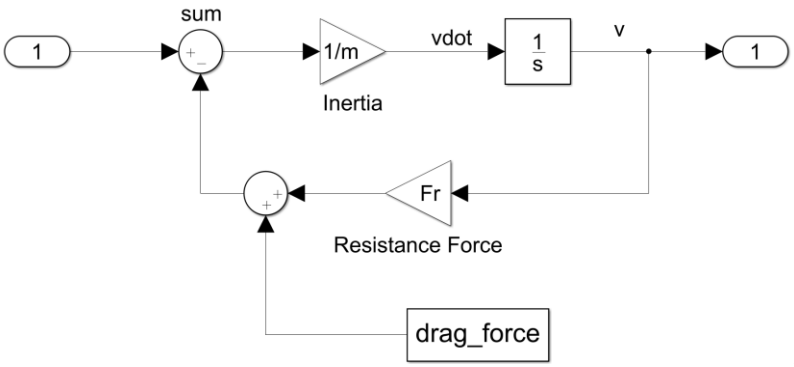

Figure 2. Plant modelling on vehicles.

several parameters in assessing motion sickness [34], but this paper only focuses on the acceleration or G force passengers feel.

RESULTS AND DISCUSSIONS

Simulation testing

The results of the vehicle CC testing on an asphalt road can be seen in Figure 3. The set point at the vehicle speed is 30.56 m/s or 110 km/hour. The time needed to reach the reference (setpoint) is 8.9 seconds. The recorded time is good for a vehicle that accommodates 7 passengers. Acceleration measurements on vehicles are also observed to see the effect of vehicle acceleration on passengers. The resulting acceleration of the vehicle can be seen in Figure 4.

Figure 4 shows that the maximum acceleration generated by the vehicle is 14.7 m/s^2 or 1.5 G. The acceleration generated by the vehicle is not too disturbing for the passengers. Humans are, on average able to withstand 5G or 49 m/s^2 of force [35]. The acceleration received by passengers is still in the comfortable category to drive; apart from that, the time when the force is applied is less than 1 second.

The next test compares the ability of CC on different road conditions. These results can be seen in Figure 5. In Figure 5, it can be seen that CC can reach the reference speed on asphalt and cobble roads, whereas, on sandy roads, CC has difficulty reaching the reference speed. The maximum speed that can be obtained by a vehicle on a sandy road is 29.91 m/s or 107.70 km/h. There is a steady-state error on sandy roads because the system cannot reach the reference speed (setpoint). The steady-state error that occurs is 2.01%; this is quite small and does not affect the vehicle or passengers much.

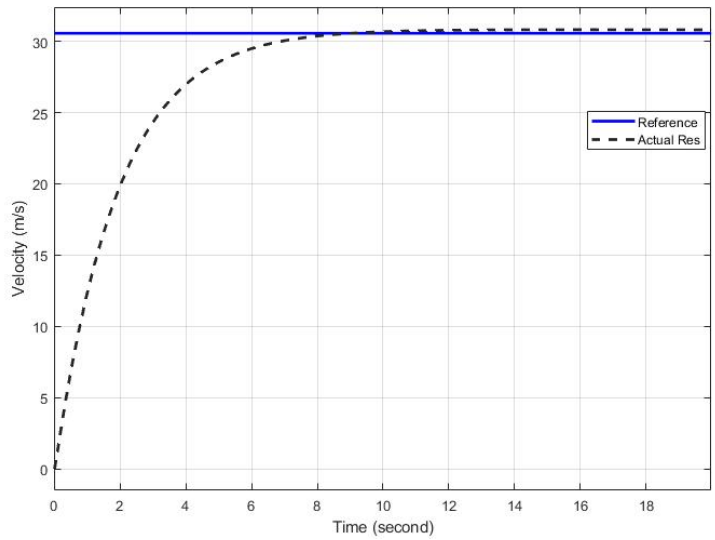

Figure 3. The results of the vehicle CC test on an asphalt road.

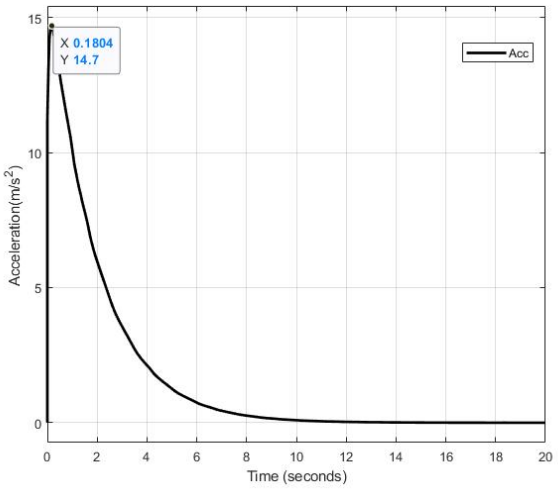

Figure 4. Acceleration generated on the vehicle.

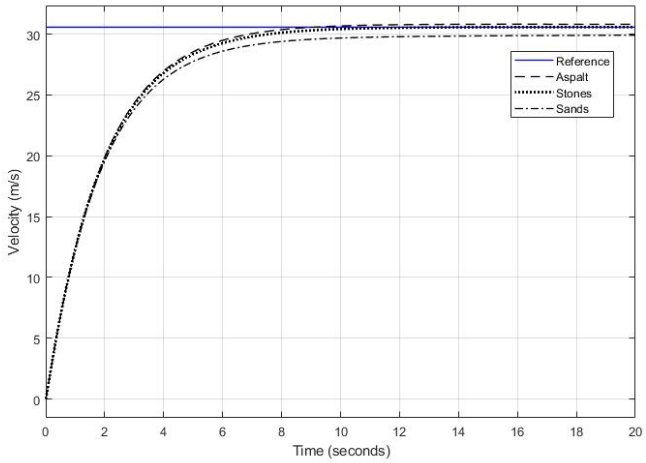

Figure 5. CC testing on asphalt, cobbles (stones) and sandy roads.

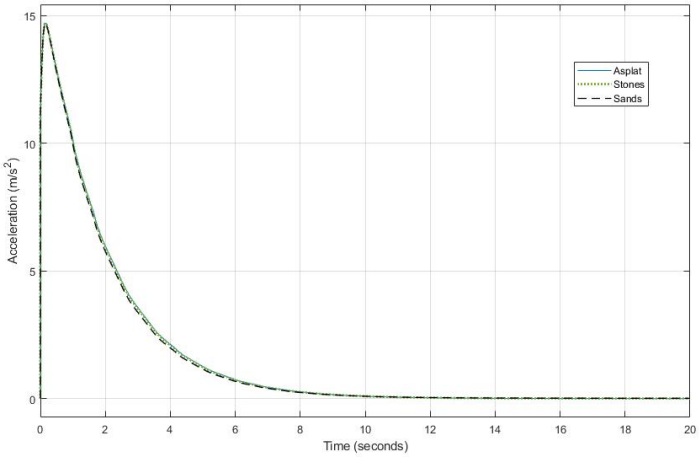

Figure 6. Measurement of vehicle acceleration on asphalt, rocky and sandy roads.

The acceleration experienced by vehicles and passengers has not changed much. The results of the acceleration test can be seen in Figure 6. Figure 6 shows that the acceleration experienced by the vehicle is almost no different between asphalt and cobble roads, but there is very little difference compared to sandy roads. Sandy roads will produce spinning on the wheels, so acceleration is slightly lower, and it is difficult to reach the desired speed, which is more difficult than asphalt and cobble roads.

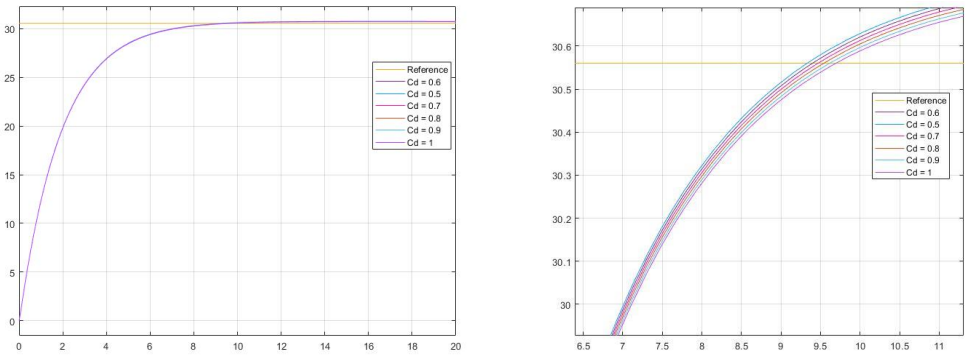

(a) (b)

Figure 7. Testing with variations in drag coefficient (C_d) (a) and (b) enlargement results from the test.

Testing with variations in the difference in drag coefficient (C_d) almost does not affect the ability of CC to reach the reference speed. Testing is done by changing the value of C_d from 0.5-1. The results of the test can be seen in Figure 7.

The results obtained in Figure 6 show that there is almost no difference even though the value of C_d is varied. This proves that the controller from CC can keep the vehicle able to adjust to the reference speed.

CONCLUSIONS

The results of the tests show that the control system design used in cruise control (CC) produces the right response and minimum steady-state error. The right response is shown by the vehicle reaching a reference speed of 110 km/h in 9 seconds; In addition, the vehicle's acceleration is not overly disruptive for both the driver and passengers. Road surface variations slightly affect the performance of the CC, but the steady-state error that occurs is only 2.01%. Testing with variations in the drag coefficient does not affect the performance of the CC. Testing the drag coefficient variation may have a big influence when the vehicle has a higher speed.

ACKNOWLEDGEMENTS

DECLARATION OF CONFLICTING INTERESTS

The author(s) declared no potential conflicts of interest with respect to the research, authorship, and/or publication of this article.

FUNDING

REFERENCES

[1] C. C. Chien and P. A. Ioannu, “Autonomous Intelligent Cruise Control,” IEEE TRANSACTIONS ON VEHICULAR TECHNOLOGY, vol. 42, no. 4, p. 16, 1993.
[2] N. Utomo, “ANALISA FAKTOR PENYEBAB KECELAKAAN LALU LINTAS PADA SEGMEN JALAN BY-PASS KRIAN – BALONGBENDO (KM. 26+000 – KM. 44+520),” vol. 2, no. 2, p. 12, 2012.
[3] H. Herawati, “Karakteristik Dan Penyebab Kecelakaan Lalu Lintas Di Indonesia Tahun 2012,” warlit, vol. 26, no. 3, p. 133, Jan. 2019, doi: 10.25104/warlit.v26i3.875.
[4] A. D. Saputra, “Studi Tingkat Kecelakaan Lalu Lintas Jalan di Indonesia Berdasarkan

Data KNKT (Komite Nasional Keselamatan Transportasi) dari Tahun 2007-2016," warlit, vol. 29, no. 2, p. 179, Jul. 2018, doi: 10.25104/warlit.v29i2.557.

[5] P. Szikora and N. Madarasz, "Self-driving cars — The human side," in 2017 IEEE 14th International Scientific Conference on Informatics, Poprad: IEEE, Nov. 2017, pp. 383–387. doi: 10.1109/INFORMATICS.2017.8327279.

[6] E. Shi, T. M. Gasser, A. Seeck, and R. Auerswald, "The Principles of Operation Framework: A Comprehensive Classification Concept for Automated Driving Functions," SAE Intl. J CAV, vol. 3, no. 1, pp. 12-03-01–0003, Feb. 2020, doi: 10.4271/12-03-01-0003.

[7] D. A. Patriawan, B. P. Natakusuma, A. A. Arifin, H. S. Maulana, and H. Irawan, "Uji Presisi dari Nonholonomic Mobile Robot pada Rancang Bangun Sistem Navigasi," Journal of Mechanical Engineering, vol. 1, p. 10, Apr. 2021.

[8] J. Fayyad, M. A. Jaradat, D. Gruyer, and H. Najjaran, "Deep Learning Sensor Fusion for Autonomous Vehicle Perception and Localization: A Review," Sensors, vol. 20, no. 15, p. 4220, Jul. 2020, doi: 10.3390/s20154220.

[9] M. Ulum, D. A. Patriawan, and M. Nizar, "Modeling and Performance Testing of Anti-Lock Braking System (ABS) with Variation of Road Friction Coefficient to Braking Distance," Rekayasa, vol. 15, no. 3, pp. 340–345, Dec. 2022, doi: https://doi.org/10.21107/rekayasa.v15i3.16561.

[10] J. Ploeg, B. T. M. Scheepers, E. van Nunen, N. van de Wouw, and H. Nijmeijer, "Design and experimental evaluation of cooperative adaptive cruise control," in 2011 14th International IEEE Conference on Intelligent Transportation Systems (ITSC), Washington, DC, USA: IEEE, Oct. 2011, pp. 260–265. doi: 10.1109/ITSC.2011.6082981.

[11] V. Milanes, S. E. Shladover, J. Spring, C. Nowakowski, H. Kawazoe, and M. Nakamura, "Cooperative Adaptive Cruise Control in Real Traffic Situations," IEEE Trans. Intell. Transport. Syst., vol. 15, no. 1, pp. 296–305, Feb. 2014, doi: 10.1109/TITS.2013.2278494.

[12] K. Sailan and Klaus. D. Kuhnert, "Modeling and Design of Cruise Control System with Feedforward for all Terrian Vehicles," in Computer Science & Information Technology (CS & IT), Academy & Industry Research Collaboration Center (AIRCC), Nov. 2013, pp. 339–349. doi: 10.5121/csit.2013.3828.

[13] J. Balkwill, Performance vehicle dynamics: engineering and applications. Butterworth-Heinemann, 2017.

[14] T. Szirtes and P. Rózsa, Eds., "CHAPTER 18 - FIFTY-TWO ADDITIONAL APPLICATIONS," in Applied Dimensional Analysis and Modeling (Second Edition), Second Edition.Burlington: Butterworth-Heinemann, 2007, pp. 527–657. doi https://doi.org/10.1016/B978-012370620-1.50024-1.

[15] J. Ai, J.-F. Chen, J. M. Rotter, and J. Y. Ooi, "Assessment of rolling resistance models in discrete element simulations," Powder Technology, vol. 206, no. 3, pp. 269–282, Jan. 2011, doi: 10.1016/j.powtec.2010.09.030.

[16] U. Sandberg et al., Rolling resistance: basic information and state-of-the-art on measurement methods. Final version. Statens väg-och transportforskningsinstitut, 2011.

[17] L. G. Andersen, J. K. Larsen, E. S. Fraser, B. Schmidt, and J. C. Dyre, "Rolling Resistance Measurement and Model Development," J. Transp. Eng., vol. 141, no. 2, p. 04014075, Feb. 2015, doi: 10.1061/(ASCE)TE.1943-5436.0000673.

[18] D. E. Hall and J. C. Moreland, "Fundamentals of Rolling Resistance," Rubber Chemistry and Technology, vol. 74, no. 3, pp. 525–539, Jul. 2001, doi: 10.5254/1.3547650.

[19] B. Wen, G. Rogerson, and A. Hartke, "Correlation Analysis of Rolling Resistance Test

Results from SAE J1269 and J2452," presented at the SAE 2014 World Congress & Exhibition, Apr. 2014, pp. 2014-01–0066. doi: 10.4271/2014-01-0066.
[20] A. Hölzer and M. Sommerfeld, "New simple correlation formula for the drag coefficient of non-spherical particles," Powder Technology, vol. 184, no. 3, pp. 361–365, Jun. 2008, doi: 10.1016/j.powtec.2007.08.021.
[21] G. I. Kelbaliyev, "Drag coefficients of variously shaped solid particles, drops, and bubbles," Theor Found Chem Eng, vol. 45, no. 3, pp. 248–266, Jun. 2011, doi: 10.1134/S0040579511020084.
[22] N.-S. Cheng, "Comparison of formulas for drag coefficient and settling velocity of spherical particles," Powder Technology, vol. 189, no. 3, pp. 395–398, 2009.
[23] R. Rajamani and C. Zhu, "Semi-autonomous adaptive cruise control systems," IEEE Trans. Veh. Technol., vol. 51, no. 5, pp. 1186–1192, Sep. 2002, doi: 10.1109/TVT.2002.800617.
[24] W. Pananurak, S. Thanok, and M. Parnichkun, "Adaptive cruise control for an intelligent vehicle," in 2008 IEEE International Conference on Robotics and Biomimetics, Bangkok: IEEE, Feb. 2009, pp. 1794–1799. doi: 10.1109/ROBIO.2009.4913274.
[25] S. Bennett, "Development of the PID controller," IEEE Control Syst., vol. 13, no. 6, pp. 58–62, Dec. 1993, doi: 10.1109/37.248006.
[26] R. P. Borase, D. K. Maghade, S. Y. Sondkar, and S. N. Pawar, "A review of PID control, tuning methods and applications," Int. J. Dynam. Control, vol. 9, no. 2, pp. 818–827, Jun. 2021, doi: 10.1007/s40435-020-00665-4.
[27] D. A. Patriawan, B. Pramujati, and H. Nurhadi, "Preliminary Study on Magnetic Levitation Modeling Using PID Control," Applied Mechanics and Materials, vol. 493, pp. 517–522, Jan. 2014, doi: 10.4028/www.scientific.net/AMM.493.517.
[28] B. Pramujati, H. Nurhadi, and D. A. Patriawan, "A Study on the Effect of an Attractive and a Repulsive Forces with Feedback Control on a Magnetic Levitation System," International Journal of Scientific & Engineering Research, vol. 6, no. 6, p. 5, 2015.
[29] [29] Z. Wang and C. Zhu, "Active Control of Active Magnetic Bearings for Maglev Flywheel Rotor System Based on Sliding Mode Control," in 2016 IEEE Vehicle Power and Propulsion Conference (VPPC), Hangzhou, China: IEEE, Oct. 2016, pp. 1–6. doi: 10.1109/VPPC.2016.7791603.
[30] W.-R. Wang, J.-H. Yan, and G.-J. Yang, "Adaptive predictive control based on ship magnetic levitation damping device," Journal of the Chinese Institute of Engineers, vol. 45, no. 2, pp. 138–149, 2022.
[31] R. Vilanova, "IMC based Robust PID design: Tuning guidelines and automatic tuning," Journal of Process Control, vol. 18, no. 1, pp. 61–70, Jan. 2008, doi: 10.1016/j.jprocont.2007.05.004.
[32] H. O. Bansal, R. Sharma, and P. R. Shreeraman, "PID Controller Tuning Techniques: A Review," Journal of Control Engineering and Technology, vol. 2, 2012.
[33] A. A. Muntashir, E. Purwanto, B. Sumantri, H. H. FAkhruddin, and R. A. N. Apriyanto, "Static and Dynamic Performance of Vector Control on Induction Motor with PID Controller: An Investigation on LabVIEW," AE, vol. 4, no. 2, pp. 83–96, May 2021, doi: 10.31603/ae.4812.
[34] M. N. A. Mohd Norzam, J. Karjanto, N. Md. Yusof, M. Z. Hassan, A. F. Hakim Zulkifli, and A. A. Ab Rashid, "Analysis of User's Comfort on Automated Vehicle Riding Simulation using Subjective and Objective Measurements," AE, vol. 5, no. 2, pp. 238–250, May 2022, doi: 10.31603/ae.6913.
[35] H. Z. Tan, B. Eberman, M. A. Srinivasan, and B. Cheng, "HUMAN FACTORS FOR THE DESIGN OF FORCE-REFLECTING HAPTIC INTERFACES," vol. 55, no. 1, pp. 353–359, 1994.